

# Short-range order, atomic dynamics, and specific heat of the amorphous Zr-Be system

A. M. Bratkovskii, S. L. Isakov, S. N. Ishmaev, I. P. Sadikov, A. V. Smirnov, G. F. Strykh, M. N. Khlopin, and N. A. Chernoplekov

*I. V. Kurchatov Institute of Atomic Energy, Moscow*

(Submitted 23 May 1991)

Zh. Eksp. Teor. Fiz. **100**, 1392–1404 (October 1991)

Detailed investigations were made of the short-range structural order, of the spectrum of atomic vibrations, and of electronic properties of the amorphous  $Zr_{1-x}Be_x$  system ( $x = 0.3-0.5$ ) using neutron scattering methods and specific heat measurements. An increase in the Be concentration in the amorphous alloy reduced the shortest distances between identical atoms, shifted and broadened the high-energy part of the vibrational spectrum, increased the Debye temperature, and lowered the density of the electron states as well as the superconducting transition temperature. An analysis of the partial radial distributions, obtained by Monte Carlo modeling, indicated that the atomic structure of the amorphous Zr-Be alloy was dominated by geometric factors (atomic "size" and the composition of the system) and there was no significant chemical ordering. The density of the vibrational states calculated by the recursion method for a structure model with a large (15 000) number of atoms reproduced well all the main features of the experimental spectra.

## 1. INTRODUCTION

The short-range structural order and the dynamics of atomic vibrations, as well as the relationship between the phonon and electron spectra of glassy metals, are attracting major interest because of the unusual properties of these metastable systems. In studies of the structural and dynamic correlations at the level of partial atomic distributions the most detailed information can be obtained by high-resolution neutron diffraction and inelastic scattering methods employing the isotopic contrast of samples (see, for example, Refs. 1–3).

We investigated amorphous Zr-Be alloys of the metal-metal type. This particular system is interesting because of the large difference between the dimensions and masses of the atoms and because it can become amorphous in a wide range of compositions, so that it is possible to identify the structural and dynamic characteristics of the individual components. Since in such cases we cannot effectively apply the isotopic substitution method in order to provide reliable interpretation of the partial distributions, it is necessary to use computer modeling methods. The metallic binding dominates in the selected system, as confirmed by the results obtained in the present study. Consequently, we can describe the structure of this alloy system by a simple model of the pair interactions and then calculate the density of the vibrational states by the recursion method, which gives results in good agreement with the experimental data.

Samples of  $Zr_{1-x}Be_x$  glassy metals with the concentrations  $x = 0.3, 0.4,$  and  $0.5$  were prepared by rapid quenching of the melt on the surface of a rotating copper disk in a helium atmosphere. Structural investigations of the short-range order were made by neutron diffraction using the time-of-flight method and a pulsed source of neutrons in the Fakel accelerator. The same amorphous alloy samples were used in a study of inelastic neutron scattering employing a spectrometer with a cold-neutron source in the IR-8 reactor and of the low-temperature behavior of the specific heat intended to reveal the phonon and electron contributions.

## 2. SHORT-RANGE STRUCTURAL ORDER

The structure factor  $S(Q)$  of amorphous  $Zr_{1-x}Be_x$  alloys with  $x = 0.3, 0.4,$  and  $0.5$  was determined over a wide range of the transferred momenta  $Q = 0.4-50 \text{ \AA}^{-1}$ . The results are presented in Fig. 1. We can see that an increase in the Be concentration considerably reduced the height of the first and second peaks of  $S(Q)$ , and it also broadened and shifted them. The behavior of the structure factor at high values of the transferred momentum was also different. In the range  $6-10 \text{ \AA}^{-1}$  the oscillations differed both in amplitude and phase. In the range  $Q > 10 \text{ \AA}^{-1}$  the oscillations became weaker, but nevertheless their inclusion was essential for reconstruction of the function representing the radial atomic distribution.<sup>2</sup>

The total reduced radial atomic distribution  $G(r)$  was found from the measured structure factors using

$$G(r) = \frac{2}{\pi} \int_0^{Q_{\max}} M(Q) Q [S(Q) - 1] \sin Qr \, dQ, \quad (1)$$

where

$$M(Q) = \sin(\pi Q/Q_{\max}) / (\pi Q/Q_{\max})$$

is a modifying function introduced to reduce the contribution of apparent oscillations in the process of the inverse Fourier transformation, needed to ensure that the final limit  $Q_{\max}$  is obtained.

Figure 2 shows the distribution functions  $G(r)$  plotted for three values of  $x$ , obtained for  $Q_{\max} = 41.5 \text{ \AA}^{-1}$ , which ensured that the resolution in the coordinate space was high ( $\Delta r = 0.13 \text{ \AA}$ ) and the random experimental errors had little effect on the function  $G(r)$  when the value of  $Q$  was high. The complete  $G(r)$  function is a weighted sum of the partial distributions of atoms  $G_{ab}(r)$ :

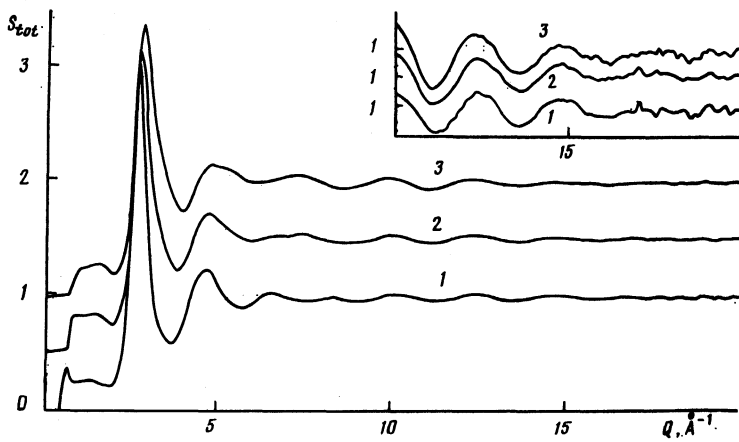


FIG. 1. Structure factor  $S(Q)$  of amorphous  $Zr_{1-x}Be_x$  alloys with  $x = 0.3$  (1),  $0.4$  (2), and  $0.5$  (3). The range  $Q > 10 \text{ \AA}^{-1}$  is shown as an inset on an enlarged scale ( $\times 5$ ).

$$G(r) = \sum_{ab} w_{ab} G_{ab}(r), \quad (2)$$

where  $w_{ab} = c_a c_b b_a b_b / \langle b^2 \rangle$ ;  $c_a$ ,  $c_b$  and  $b_a$ ,  $b_b$  are the concentrations and amplitudes of the coherent neutron scattering by the  $a$  and  $b$  (Zr and Be) atoms;

$$\langle b^2 \rangle = (1-x)b_{Zr}^2 + x b_{Be}^2, \quad (3)$$

$$b_{Zr} = 0.716 \cdot 10^{-12} \text{ cm}, \quad b_{Be} = 0.779 \cdot 10^{-12} \text{ cm}.$$

In view of the similarity of the scattering amplitudes of Zr and Be, the coefficients  $w_{ab}$  are comparable and, if we allow for the considerable difference between the sizes of the

atoms, we find that the complete function  $G(r)$  includes the contributions of all the partial distributions: Zr-Zr, Be-Zr, Be-Be. Using an expansion in three Gaussians in the first coordination sphere, we determined the shortest interatomic distances  $r_{ab}$  listed in Table I. An analysis of these distances demonstrates that the distances  $r_{Be-Be}$  and  $r_{Zr-Zr}$  in the Zr-Be system are less than the "diameters" of the corresponding atoms in pure metals ( $2R_{Be} = 2.28 \text{ \AA}$  and  $2R_{Zr} = 3.23 \text{ \AA}$ ), whereas the third distance obeys  $r_{Zr-Be} > \frac{1}{2}(r_{Be-Be} + r_{Zr-Zr})$ . An increase in the Be concentration results in a tendency to shorten the distances between the like atoms without altering the distance  $r_{Zr-Be}$ . Table I lists also the atomic densities  $n$  of amorphous alloys determined by the Archimedes method for the compositions  $x = 0.3$  and  $0.4$ , as well as the packing factor

$$\eta = \frac{4\pi}{3} [(1-x)R_{Zr}^3 + xR_{Be}^3] n. \quad (4)$$

The packing factors  $\eta$  have values typical of amorphous metallic alloys ( $\sim 0.7$ ) and decrease somewhat as the concentration of smaller atoms increases.

It is difficult to interpret the experimental data on the basis of the partial contributions. Therefore, we investigated the structure of our amorphous alloys in computer experiments which were carried out using the classical Monte Carlo method and an isochoric ensemble of  $N = 500$  particles placed inside a cube of volume  $V$  with periodic boundary conditions (the values of the atomic volume  $V/N$  agreed with the experimental data). The actual implementation of the modeling method was described in Refs. 4 and 5. The Morse pair central potential with a cutoff function  $f(x)$  was used to describe the effective interaction between atoms:

$$\varphi_{ab}(r) = \varepsilon_{ab} \{ \exp[-2\alpha(r/\sigma_{ab}-1)] - 2 \exp[-\alpha(r/\sigma_{ab}-1)] \} f(r/\sigma_{ab}), \quad (5)$$

where  $\varepsilon_{BeBe}/\varepsilon_{ZrZr} = 0.55$ ,  $\sigma_{ZrZr} = 3.18 \text{ \AA}$ ,  $\sigma_{BeBe} = 2.28 \text{ \AA}$ ,  $\varepsilon_{ZrBe} = (\varepsilon_{BeBe} \varepsilon_{ZrZr})^{1/2}$ ,  $\sigma_{ZrBe} = (\sigma_{ZrZr} + \sigma_{BeBe})/2$ , and  $\alpha = 4.53$ . This choice of the parameters for the interatomic potentials in Eq. (5) provided a satisfactory description of the experimental total reduced radial distribution functions  $G(r)$  of amorphous Zr-Be alloys in a wide range of compositions [see Fig. 2: the positions and amplitudes of all the main peaks of  $G(r)$  were reproduced well]. The ratios of the depths of the Zr-Zr and Be-Be potentials were selected on the basis of the cohesive energies of the corresponding ele-

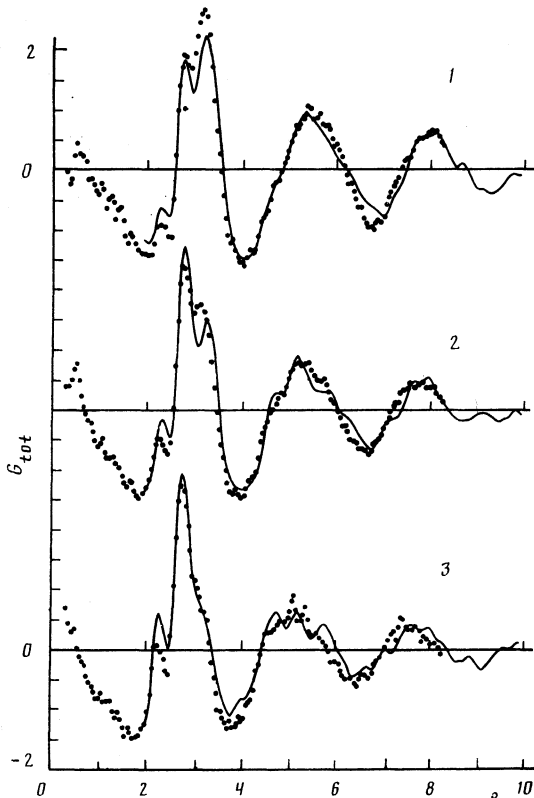


FIG. 2. Total reduced radial distribution function  $G(r)$  of amorphous  $Zr_{1-x}Be_x$  alloys with  $x = 0.3$  (1),  $0.4$  (2), and  $0.5$  (3). The points are the experimental values and the curves are calculated.

TABLE I. Interatomic distances, density  $n$ , and packing factor  $\eta$  for the amorphous  $Zr_{1-x}Be_x$  system.

$x$	$r_i, \text{\AA}$			$n \cdot 10^3, \text{\AA}^{-3}$	$\eta$
	Be-Be	Be-Zr	Zr-Zr		
0,3	2,25	2,71	3,12	4,96	0,71
0,4	2,22	2,71	3,10	5,23	0,68
0,5	2,18	2,71	3,06	5,52 *	0,66

\*Calculated from Eq. (3) using the extrapolated value of  $\eta$ .

ments, the positions of the minima of these potentials were practically identical with the "diameters" of the investigated atoms, whereas the ratio  $\alpha/\sigma_{ZrZr}$  was close to a similar quantity used for metals in modeling the structure of amorphous Ni-Be and Fe-B alloys.<sup>4,6,7</sup> An obvious shortcoming of this structural model was an overestimate of the maximum  $G(r)$  corresponding to the first Be-Be coordination sphere, indi-

cating that the method used to describe the interaction of the Be atoms was not quite satisfactory.

The calculated partial reduced radial distribution functions  $G_{ab}(r)$  are plotted in Fig. 3. An analysis of these curves demonstrates that the main structural changes associated with the increasing Be concentration in the alloy were due to deformation of the split wide second maximum of  $G_{ab}(r)$

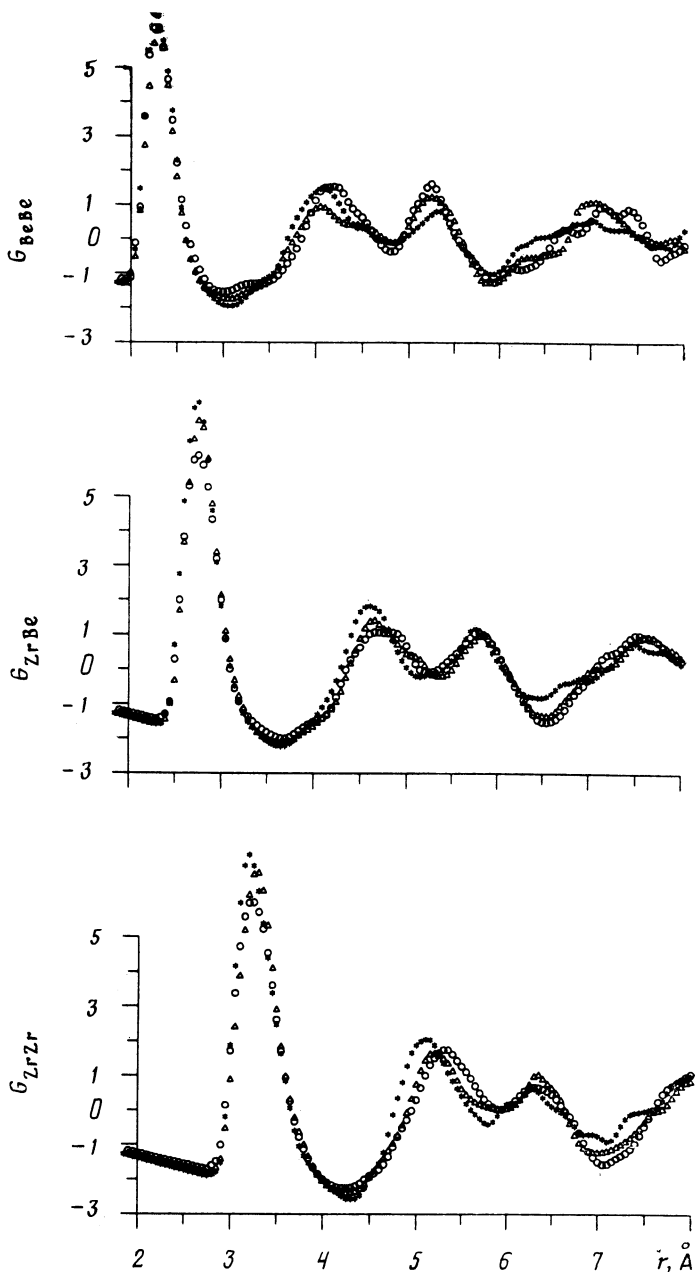


FIG. 3. Partial reduced radial distribution functions  $G_{ab}(r)$  obtained using the structure model of amorphous  $Zr_{1-x}Be_x$  alloys with  $x = 0.3$  ( $\circ$ ),  $0.4$  ( $\Delta$ ), and  $0.5$  ( $*$ ).

TABLE II. Coordination numbers for the amorphous  $Zr_{1-x}Be_x$  system. Each pair of values represents the structure model/estimate based on Eq. (7).

$x$	$Z_{ZrZr}$	$Z_{ZrBe}$	$Z_{BeZr}$	$Z_{BeBe}$	$Z_{Zr}$	$Z_{Be}$	$\langle Z \rangle$
0,3	10,9/10,4	3,2/3,0	7,3/7,1	2,2/0,7	14,1/13,4	9,5/7,8	12,7/11,7
0,4	10,0/9,7	4,5/4,4	6,8/6,6	2,7/1,5	14,5/14,1	9,5/8,1	12,5/11,7
0,5	8,9/8,7	6,2/6,1	6,2/6,1	3,9/2,5	15,1/14,8	10,1/8,6	12,5/11,7

and a slight increase of the splitting. The ratios of the positions of the subpeaks of the second maximum ( $r'_2$ ,  $r''_2$ ) had the following values:  $r'_2/r_1 \sim 1.6$  for Zr–Zr, 1.7 for Zr–Be, 1.8 for Be–Be and  $r''_2/r_1 \sim 1.95$  for Zr–Zr, 2.1 for Zr–Be, and 2.3 for Be–Be. Here,  $r_1$  is the position of the first maximum in the investigated distribution (for dense tetrahedral packing of identical spheres, we have  $r'_2/r_1 = 1.7$  and  $r''_2/r_1 = 2.0$ ). The partial functions were used to calculate the coordination numbers

$$Z_{ab} = c_b \int_{r_{min}}^{r_{max}} [4\pi r^2 n + r G_{ab}(r)] dr, \quad (6)$$

where  $r'_{min}$  and  $r''_{min}$  are the positions of the minima  $G_{ab}(r)$  in the first coordination sphere. The results are presented in Table II. This table gives estimates of the coordination numbers deduced from the following phenomenological relationship<sup>8</sup>

$$z_{ab} = c_b n_0 \Omega (R_a + R_b)^3 - \delta_{ab}, \quad (7)$$

describing well the experimental data for a large number of binary amorphous alloys if  $\Omega \approx 9.2$ , and the density  $n_0$  corresponds to the packing factor  $\eta_0 = 0.75$ , which usually underestimates somewhat the values of  $Z_{ab}$ . It is worth pointing out the similarity of the values of  $Z_{ZrZr}$  and  $Z_{ZrBe}$  in the structure model and those deduced from Eq. (7). On the other hand, the values of  $Z_{BeBe}$  differ significantly. Computer modeling is known to overestimate the value of  $Z_{BeBe}$  compared with the experimental data. This is due to the above-mentioned difference  $G(r)$  in the first coordination sphere.

In an analysis of the chemical short-range order it is useful to employ a generalized parameter  $\alpha_w/\alpha_w^{max}$  (Ref. 9), defined in terms of the coordination numbers:<sup>10</sup>

$$\alpha_w = \frac{Z_{cc}}{Z_w}, \quad \alpha_w^{max} = -\frac{\min(c_1, c_2)}{\max(c_1, c_2)}, \quad (8)$$

where

$$Z_{cc} = z_2(Z_{11} - Z_{21}) + c_1(Z_{22} - Z_{12}), \quad Z_w = c_2 Z_1 + c_1 Z_2,$$

and the indices 1 and 2 apply to Zr and Be, respectively. The negative or positive values of  $\alpha_w/\alpha_w^{max}$  indicate that the local environment is occupied preferentially by atoms of unlike (like) types, whereas the condition  $\alpha_w/\alpha_w^{max} = 0$  corresponds to the complete absence of the chemical short-range order in the local environment. A calculation of this parameter for the investigated alloys gives the following values:  $\alpha_w/\alpha_w^{max} = -0.075$  ( $Zr_{70}Be_{30}$ ),  $-0.021$  ( $Zr_{60}Be_{40}$ ), and  $-0.017$  ( $Zr_{50}Be_{50}$ ). The low values of the parameter

$\alpha_w/\alpha_w^{max}$  indicate the absence of a significant chemical ordering in the system being modeled, particularly in the case of the alloys with high Be concentrations. The same conclusion follows from an analysis of these parameters calculated from the coordination numbers defined by Eq. (7).

### 3. VIBRATIONAL SPECTRUM

Information on the density of the vibrational states of the  $Zr_{1-x}Be_x$  system was obtained by the inelastic neutron scattering method employing a multidetector time-of-flight spectrometer with a cold neutron source.<sup>11</sup> The energy and broadening of the lines of the neutrons incident on a sample were, respectively,  $E_0 \approx 4.8$  meV and  $\Delta E_0/E_0 \approx 10\%$ . An analysis of the experimental data made it possible to reconstruct the generalized density of the vibrational states  $G(E)$  representing the sum of the partial distributions of the vibrational states  $g_a(E)$  of the Zr and Be atoms with appropriate weighting factors:<sup>12</sup>

$$\frac{d^2\sigma}{d\Omega dE} \sim G(E) = \sum_a w_a \exp(-2W_a) g_a(E), \quad (9)$$

where

$$w_a = \frac{c_a \sigma_a}{m_a} / \sum_a \frac{c_a \sigma_a}{m_a},$$

$c_a$ ,  $\sigma_a$ , and  $m_a$  are the concentrations, scattering cross sections, and the masses of the nuclei of the elements in our samples;  $\exp(-2W_a)$  is the Debye–Waller factor.

The values of the weighting factors  $w_{Be}$  are 0.823, 0.882, and 0.923 for  $x = 0.3$ , 0.4, and 0.5, respectively. Therefore, the main contribution to  $G(E)$  comes from the vibrations of the Be atoms. The reconstructed normalized  $G(E)$  spectra for the range of  $E$  from 1.5 to 80 meV are plotted in Fig. 4. We can see that the spectral density of the vibrations splits into two clearly separate regions: 0–28 and 28–80 meV. An increase in the concentration of the light Be atoms reduces the density of states in the low-energy part of the  $G(E)$  spectrum and increases the density of the high-energy vibrations in the range  $E > 50$  meV. The changes in the high-energy part of the spectrum are a shift of the maximum from 52 to 54 meV and an increase in the half-width of the distribution from 26 to 32 meV.

We calculated the vibrational spectra for structural models of the investigated amorphous alloys. The calculations were carried out by a recursive method<sup>13</sup> which is most effective in the case of disordered systems. In this method the density of the vibrational states was found by statistical averaging, over the amorphous system, of the imaginary part of the local Green's function  $G_{ii}(E^2) = \langle i | (E^2 - \mathbf{D})^{-1} i \rangle$  ( $\mathbf{D}$  is a dynamic matrix) associated with vibrations of an atom  $i$ , which can be calculated using a continued fraction:

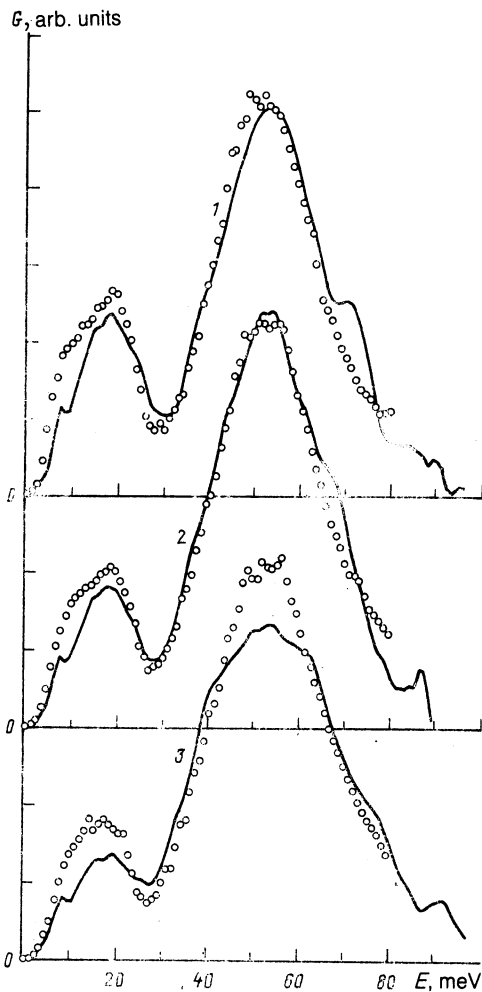


FIG. 4. Generalized vibrational spectrum of atoms  $G(E)$  in the amorphous  $Zr_{1-x}Be_x$  system with  $w = 0.3$  (1),  $0.4$  (2), and  $0.5$  (3) (experimental results).

$$g(E) = \frac{1}{3N} \sum_i g_{ii}(E), \quad (10)$$

$$g_{ii}(E) = -\frac{1}{\pi} \lim_{\epsilon \rightarrow 0} \text{Im} [2EG_{ii}(E^2 + i\epsilon)],$$

$$G_{ii} = \frac{1}{E^2 - a_1 - b_1^2} \frac{1}{E^2 - a_2 - b_2^2} \dots \quad (11)$$

Here,  $N$  is the number of atoms participating in the averaging procedure (in real calculations the summation is usually carried out over a part of the investigated system, which in our calculations was  $N = 75$ ); the coefficients  $a_n$  and  $b_n$  are described by the following recursion relation:

$$a_n = \langle n-1 | \mathbf{D} | n-1 \rangle, \quad b_n = \langle n | \mathbf{D} | n-1 \rangle, \quad b_0 = 0, \quad (12)$$

$$b_n | n \rangle = (\mathbf{D} - a_n) | n-1 \rangle - b_{n-1} | n-2 \rangle,$$

the vectors  $|0\rangle \equiv |i\rangle, |1\rangle, \dots, |n\rangle, \dots$  form an orthonormalized set of states. In view of the limited computer capacity, we calculated 15 pairs of the recursion coefficients ( $a_n, b_n$ )

and constructed  $g(E)$  using the quadratic Gaussian approximation suggested by Nex.<sup>14</sup>

The generalized densities of states  $G(E)$  obtained in this way are plotted alongside the experimental data in Fig. 5, where the absolute value of the depth of the potential  $\epsilon_{ZrZr}$  is selected to be  $0.52$  eV. The agreement with the experiments is satisfactory: on the whole, the calculations provide a correct description of the main singularities of  $G(E)$  and their variation with the composition of the alloy, but there are significant differences in details.

Figure 6 gives the partial vibrational densities of states  $g(E)$  for Zr and Be. It shows that the low-energy part of the total vibrational density of states is governed by the vibrations of the Zr atoms and the high-energy part is associated with the Be atoms. The reduction in the density of states  $G(E)$  with increasing Be concentration at energies  $10$ – $25$  meV is explained primarily by a simple change in the weighting coefficient, although an increase in the difference between the experimental (Fig. 4) and calculated (Fig. 6) spectra is evidence that the partial densities of states depend on the composition of the alloy in this range of values of  $E$ . The calculated curves show practically no such dependence. The broadening of the curve representing the total density of states on increase in  $c_{Be}$  is entirely due to the sensitivity of  $g_{Be}(E)$  to the ratio of the components in the system.

We must mention also that the Zr–Be interaction hardly affects the density of the Zr states, in spite of the large value of the coordination number  $Z_{ZrBe}$ , particularly in the case of the alloy  $Zr_{50}Be_{50}$ . The considerable difference between the calculated and experimental maxima of the vibrational densities of states in the amorphous alloy  $Zr_{50}Be_{50}$  is clearly due to sufficiently accurate selection (for this alloy composition) of the effective interaction between the atoms, as pointed out already in an analysis of the structural model. If the experimental data are analyzed using the results of our calculations, it is found that at low energies ( $< 10$  meV) the density of the Zr vibrations clearly decreases as a result of an increase in the Be concentration from  $0.3$  to  $0.5$ .

The inaccuracies in the behavior of the calculated vibrational spectra may be due, in particular, to the electron contributions ignored in our simple model. Consequently, we investigated the dependence of the density of the electron states on the composition in these systems by measuring the specific heat.

#### 4. SPECIFIC HEAT

The specific heat of our samples was determined in the temperature range  $1.6$ – $40$  K in magnetic fields  $0$  and  $4$  T. The measurements were made by an adiabatic method<sup>16</sup> and the error was of the order of  $2\%$ . The results are presented in Fig. 7 and in Tables III and IV.

In the absence of a magnetic field the temperature dependence of the specific heat of  $Zr_{0.7}Be_{0.3}$  and  $Zr_{0.6}Be_{0.4}$  samples exhibited an abrupt jump corresponding to the superconducting transition. A magnetic field of  $4$  T suppressed the superconductivity, which made it possible to determine the specific heat in the normal (nonsuperconducting) state right down to the lowest temperatures. Below  $12$  K, the temperature dependence of the specific heat was described satisfactorily by the usual law for metals:  $C = \gamma T + \beta T^3$ , corre-

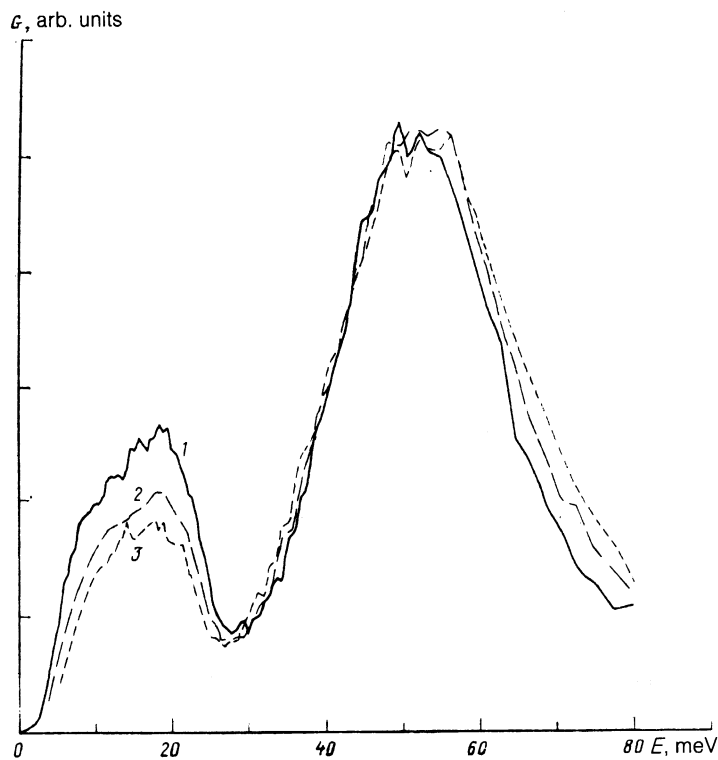


FIG. 5. Comparison of the experimental (circles) and calculated (continuous curves)  $G(E)$  spectra of amorphous  $Zr_{1-x}Be_x$  alloys with  $x = 0.3$  (1),  $0.4$  (2), and  $0.5$  (3).

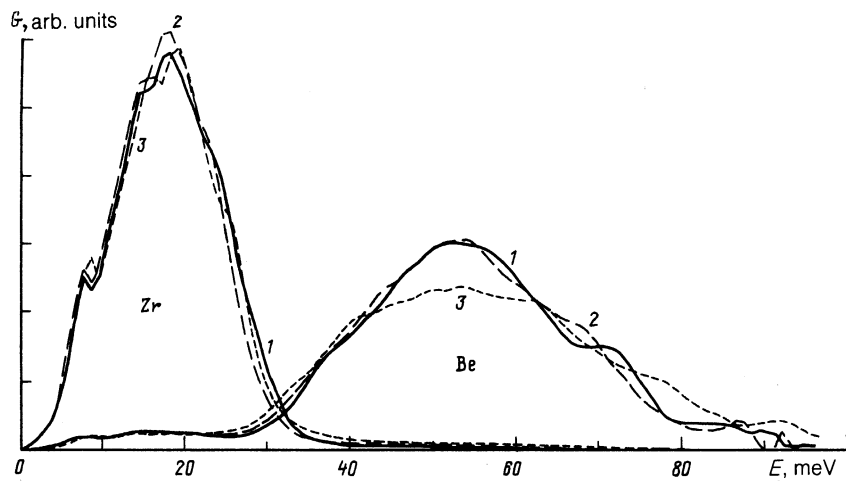


FIG. 6. Partial densities of states  $g_{Zr}(E)$  and  $g_{Be}(E)$  for the amorphous  $Zr_{1-x}Be_x$  system. The curves are calculated using the structure model for  $x = 0.3$  (1),  $0.4$  (2), and  $0.5$  (3).

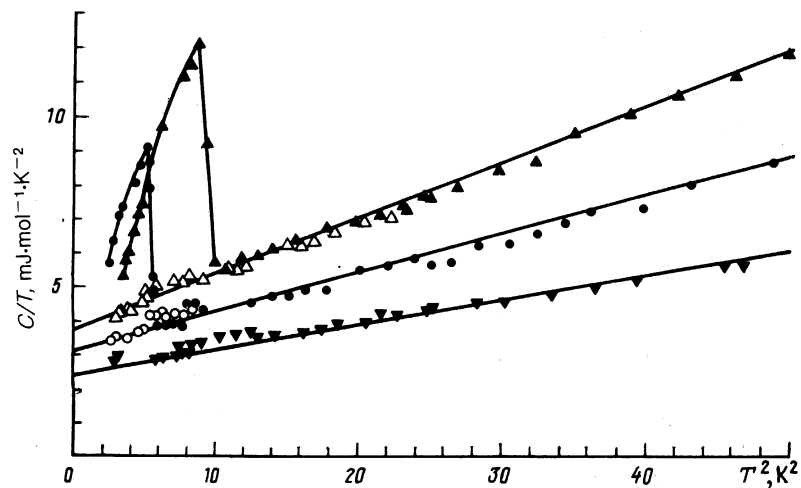


FIG. 7. Temperature dependences of the specific heat of amorphous  $Zr_{1-x}Be_x$  alloys in the absence of a magnetic field ( $\nabla$ ,  $\circ$ ,  $\blacktriangle$ ) and in a magnetic field of  $4$  T ( $\circ$ ,  $\Delta$ ):  $\nabla$ )  $Zr_{0.5}Be_{0.5}$ ;  $\circ$ ),  $\bullet$ )  $Zr_{0.6}Be_{0.4}$ ;  $\Delta$ ),  $\blacktriangle$ )  $Zr_{0.7}Be_{0.3}$ .

TABLE III. Smoothed-out values of the specific heat of amorphous  $Zr_{1-x}Be_x$  alloys in the normal (nonsuperconducting) state ( $J \cdot mol^{-1} \cdot K^{-1}$ ).

T, K	$Zr_{0.5}Be_{0.5}$	$Zr_{0.6}Be_{0.4}$	$Zr_{0.7}Be_{0.3}$
2	0,0054	0,0072	0,0088
5	0,0216	0,030	0,040
10	0,099	0,151	0,207
15	0,301	0,447	0,593
20	0,654	0,927	1,20
25	1,16	1,57	2,00
30	1,83	2,38	2,95
35	2,58	3,33	4,02
40	3,30	4,08	5,08

sponding to a straight line when plotted using the coordinates  $C/T$  and  $T^2$ .

The values of the parameters  $\gamma$  and  $\beta$  determined by the least-squares method are listed in Table IV. The first (linear) term in the above expression represents the specific heat of the electron system. The value of the Sommerfeld coefficient  $\gamma$  in this term is proportional to the density of the electron states at the Fermi level. We can see that both the coefficient  $\gamma$  and the specific heat jump  $\Delta C/T$  are larger for samples with higher zirconium concentrations, demonstrating that the density of the electron states increases with the zirconium concentration.

The cubic term represents the specific heat of the phonon system and its magnitude is related to the characteristic Debye temperature  $\Theta$ :  $\beta = 12\pi^4 R / 5\Theta^3$ , where  $R$  is the gas constant. We can see that the value of the Debye temperature increases with the beryllium content and estimates show that the observed increase in this temperature is greater than that predicted by the model ignoring the change in the interaction force between the atoms. This can be explained by assuming that the constants of the interaction force in the lattice increase with the beryllium content. One of the possible reasons for this stiffening of the lattice may be the screening influence of the electrons, which decreases as the density of the electron states at the Fermi level is reduced.<sup>17</sup> It should be pointed out that our values of the coefficients  $\gamma$  and  $\beta$  are somewhat less than those reported in Refs. 18 and 19 for freshly prepared samples. In contrast to Refs. 18 and 19, we investigated heat-treated samples, and the difference could be due to a reduction in the density of the electron phonon states caused by structural relaxation induced by the heat treatment.<sup>20</sup>

## 5. CONCLUSIONS

We investigated the structure factor of the amorphous  $Zr_{1-x}Be_x$  ( $x = 0.3, 0.4,$  and  $0.5$ ) system up to transferred momentum values  $50 \text{ \AA}^{-1}$  and reconstructed the complete

radial distribution functions, for which the partial distributions of atoms in the first coordination sphere were manifested. This made it possible to determine the shortest interatomic distances which in the case of the like atoms tended to shorten as the Be concentration rose, but were practically unaffected by this concentration in the case of the Zr-Be pairs. The generalized spectra of the atomic vibrations were determined for the same amorphous alloys. The spectra were found to split into two characteristic regions corresponding to the predominant vibrations of the light and heavy atoms. An increase in the Be concentration shifted and broadened the high-energy part of the spectrum, which was in agreement with the nature of changes in the interatomic distances.

The Monte Carlo method was used to construct a model of the amorphous Zr-Be system with the interatomic pair central potentials of the Morse type, which was capable of reproducing the experimental data on the structural short-range order and on the dynamics of the atomic vibrations throughout the investigated range of compositions. This made it possible to interpret the results at the level of the structural and dynamic partial distributions. An analysis of the chemical short-range order parameter on the basis of the coordination numbers indicated that there was no significant chemical ordering in the amorphous Zr-Be system. The partial spectra of the Be and Zr vibrations, calculated by the recursive method, differed qualitatively: the vibrations of the Zr atoms were localized mainly in the low-energy part of the spectrum, whereas the vibrational states of Be were distributed not only in the high-energy part, but had a significant density at low frequencies. However, it should be pointed out that one shortcoming of our model was a somewhat unsatisfactory description of the interaction of the Be atoms.

We determined the specific heat and the values of the Sommerfeld coefficient  $\gamma$ , the characteristic Debye temperature  $\Theta$ , and the temperature of the superconducting transition  $T_c$ . An increase in the beryllium content reduced the density of the electron states and the superconducting transition temperature, but increased the Debye temperature.

TABLE IV. Characteristics of the superconducting transition, and of the phonon and electron spectra of amorphous alloys deduced from the specific heat data.

Alloy	$T_c, K$	$\Delta C/T_c,$ $mJ \cdot K^2 \cdot mol^{-1}$	$\gamma,$ $mJ \cdot K^2 \cdot mol^{-1}$	$\beta,$ $mJ \cdot K^4 \cdot mol^{-1}$	$\Theta, K$
$Zr_{0.5}Be_{0.5}$	—	—	2,38	0,077	293
$Zr_{0.6}Be_{0.4}$	2,35	5,5	3,11	0,118	254
$Zr_{0.7}Be_{0.3}$	3,05	7,2	3,71	0,169	228

Two of the present authors (A. M. Bratkovskii and A. V. Smirnov) regard it as their pleasant duty to thank Dr. Chris Nex for his help in this investigation and for information on the method described in Ref. 15.

- <sup>1</sup> S. N. Ishmaev, S. L. Isakov, I. P. Sadikov *et al.*, *J. Non-Cryst. Solids* **94**, 11 (1987).
- <sup>2</sup> E. Sváb and S. N. Ishmaev, *Proc. Fifth Intern. School on Neutron Physics, Alushta, 1986*, publ. by Joint Institute of Nuclear Research, Dubna (1987), p. 287.
- <sup>3</sup> M. G. Zemlyanov, G. F. Syrykh, N. A. Chernoplekov, and É. Shvab, *Zh. Eksp. Teor. Fiz.* **94**(11), 365 (1988) [*Sov. Phys. JETP* **67**, 2381 (1988)].
- <sup>4</sup> A. M. Bratkovsky and A. V. Smirnov, *Phys. Lett. A* **146**, 522 (1990).
- <sup>5</sup> A. M. Bratkovskii and A. V. Smirnov, *Rasplavy* No. 1, 32 (1990).
- <sup>6</sup> D. O. Welch, G. J. Dienes, and A. Paskin, *J. Phys. Chem. Solids* **39**, 589 (1978).
- <sup>7</sup> T. Fujiwara, H. S. Chen, and Y. Waseda, *J. Phys. F* **11**, 1327 (1981).
- <sup>8</sup> S. L. Isakov and S. N. Ishmaev, *Vopr. At. Nauki Tekh. Ser. Yadernofiz. Issled. Teor. Eksp. No. 5*(13), 27 (1990).
- <sup>9</sup> B. E. Warren, *X-Ray Diffraction*, Addison-Wesley, Reading, MA (1969).
- <sup>10</sup> R. Harris and L. J. Lewis, *J. Phys. F* **13**, 1359 (1983).
- <sup>11</sup> M. G. Zemlyanov, A. E. Golovin, S. P. Mironov *et al.*, *Prib. Tekh. Eksp. No. 5*, 34 (1973).
- <sup>12</sup> N. A. Chernoplekov, M. G. Zemlyanov, E. G. Brovman, and A. G. Checherin, *Fiz. Tverd. Tela (Leningrad)* **5**, 112 (1963) [*Sov. Phys. Solid State* **5**, 78 (1963)].
- <sup>13</sup> R. Haydock, *Solid State Phys.* **35**, 215 (1980).
- <sup>14</sup> C. M. M. Nex, *J. Phys. A* **11**, 653 (1978).
- <sup>15</sup> C. M. M. Nex, *Comput. Phys. Commun.* **34**, 101 (1984).
- <sup>16</sup> M. N. Khlopkin, N. A. Chernoplekov, and P. A. Cheremnykh, Preprint No. IAÉ-3549/10 [in Russian], Kurchatov Institute of Atomic Energy, Moscow (1982).
- <sup>17</sup> G. F. Syrykh, M. G. Zemlyanov, N. A. Chernoplekov, and B. I. Savel'ev, *Zh. Eksp. Teor. Fiz.* **81**, 308 (1981) [*Sov. Phys. JETP* **54**, 165 (1981)].
- <sup>18</sup> G. Kh. Panova, N. A. Chernoplekov, A. A. Shikov *et al.*, *Zh. Eksp. Teor. Fiz.* **88**, 1012 (1985) [*Sov. Phys. JETP* **61**, 595 (1985)].
- <sup>19</sup> G. Kh. Panova, B. I. Savel'ev, M. N. Khlopkin *et al.*, *Zh. Eksp. Teor. Fiz.* **85**, 1308 (1983) [*Sov. Phys. JETP* **58**, 759 (1983)].
- <sup>20</sup> G. F. Syrykh, *Zh. Eksp. Teor. Fiz.* **96**, 1454 (1989) [*Sov. Phys. JETP* **69**, 824 (1989)].

Translated by A. Tybulewicz